

Model Molecular Magnets

Ernest R. Davidson* and Aurora E. Clark

Department of Chemistry, Indiana University, Bloomington, Indiana 47405

Received: May 16, 2002

The local spin method suggested previously for defining the spin state of an atom in a molecule is applied to model manganese complexes with three and four manganese centers. This method extracts from the wave function a spin for the manganese centers that has been compared to the one suggested by chemical intuition. Density functional theory (DFT) calculations with various total spin projections in the “up” direction, M , but controlled $|M|$ for each manganese center, gave a set of energies that were fit to the Heisenberg Hamiltonian. The eigenvalues of this model Hamiltonian then predict the ground spin state and the preferred combinations of spin orientations of the manganese centers. In some model complexes, changes in the wave function for each spin solution made the Heisenberg Hamiltonian unsuitable for fitting. For a dinuclear manganese complex, complete active space self-consistent field calculations were performed and are in reasonable agreement with the DFT results.

Introduction

Transition metal complexes that contain multiple manganese centers have been a source of increased interest in both the theoretical and experimental communities.¹ Much of this interest has stemmed from the propensity of Mn aggregates to possess a ground-state spin that is nonzero. Such “molecular magnets” arise from either ferromagnetic interactions between some if not all of the Mn atoms and/or spin frustration effects. The temperature dependence of the magnetic susceptibility of these complexes is often fit to energy levels predicted by a Heisenberg model Hamiltonian

$$H = E_0 + \sum J_{AB} \mathbf{S}_A \cdot \mathbf{S}_B \quad (1)$$

In this equation, it is assumed that the molecule contains a few magnetic centers and that a family of states is to be described by coupling these spins with no other changes in the electronic structure. The exchange parameters, J , are specific to this one family of states and would change for other states of the molecule. It is assumed that each magnetic center has a well-defined spin S_A so that the eigenvalue of S_A^2 is $S_A(S_A + 1)$ for all states within this family. Usually, S_A is assigned by chemical intuition based on formal oxidation numbers.

The eigenfunctions of eq 1 may be expanded in the basis of states formed as the antisymmetrized direct product of the eigenstates $|S_A M_A\rangle$ of S_A^2 and S_{zA} associated with each center. Each of these, in turn, may be regarded as a linear combination of Slater determinants formed by powers of a step-down operator acting on the single Slater determinant represented by $|S_A S_A\rangle$. For a molecule with four $d^5 S = 5/2$ transition metal centers, the Heisenberg Hamiltonian will have a total of $6^4 = 1296$ eigenstates involving a total of $2^{20} = 1\,048\,576$ Slater determinants. Only the simplest one of these eigenstates with S and M both equal to 10 can be expressed by a single Slater determinant. Few electronic structure programs are capable of doing a complete active space self-consistent field (CASSCF)

calculation for the other low-spin states in this example with 20 electrons in 20 singly occupied orbitals.

The standard theoretical approach to this problem is to follow the example of Noodleman² and replace eq 1 with

$$E_X = E_0 + \sum J_{AB} \langle \mathbf{S}_A \cdot \mathbf{S}_B \rangle_X \quad (2)$$

where the subscript X denotes the approximate method used in the calculation. This method uses a sequence of calculations with single Slater determinants that are not even approximately eigenfunctions of S^2 , but are still eigenfunctions of S_z with eigenvalues M and are approximately eigenfunctions of all of the S_A^2 and S_{zA} with eigenvalues $S_A(S_A + 1)$ and $\pm S_A$, respectively. Often density functional theory (DFT) energies are used even though DFT provides only a total density and not a wave function. If it is possible to obtain energies for a sufficient number of such X , with the rest of the wave function essentially unchanged, then eq 2 can be regarded as a set of linear equations for the exchange couplings, J_{AB} . To solve these equations, it is first necessary to assign values to $\langle \mathbf{S}_A \cdot \mathbf{S}_B \rangle_X$. If $\mathbf{S}_A \cdot \mathbf{S}_B$ is written in the form

$$\mathbf{S}_A \cdot \mathbf{S}_B = S_{zA} S_{zB} + (S_{+A} S_{-B} + S_{-A} S_{+B})/2 \quad (3)$$

then it is clear that $\langle \mathbf{S}_A \cdot \mathbf{S}_B \rangle_X$ for $A \neq B$ is equal to $M_A M_B$ for any wave function with well-defined values of S_A , M_A , S_B , and M_B . Summing these averages over all A and B gives $\langle S^2 \rangle$ equal to $M^2 + S_{\max}$, where S_{\max} is the maximum value of S and is the sum of the S_A . This value of $\langle S^2 \rangle$ will usually differ somewhat from the actual average computed with the spin-unrestricted Slater determinant because of spin polarization in the approximate wave function. Alternatively, when only two radical centers are involved, it is common to replace $\mathbf{S}_A \cdot \mathbf{S}_B$ with $(S^2 - S_A^2 - S_B^2)/2$ so that

$$\langle \mathbf{S}_A \cdot \mathbf{S}_B \rangle = [\langle S^2 \rangle - S_A(S_A + 1) - S_B(S_B + 1)]/2 \quad (4)$$

and $\langle S^2 \rangle$ is evaluated with the same wave function as the energy.

Hence, this approach requires a method for extracting the values of each $\langle \mathbf{S}_A \cdot \mathbf{S}_B \rangle_X$ from a wave function. To do this, we

* To whom correspondence should be addressed. Email: davidson@indiana.edu.

need to replace the phenomenological spin operators S_A with operators acting on the electron coordinates so that average values from electronic wave functions can be computed.

In a previous publication,³ we suggested that a set of Hermitian one-electron position-space projection operators, $P_A(i)$ associated with atomic centers could be defined so that

$$P_A P_B = \delta_{AB} P_A \quad (5)$$

and

$$\sum P_A = 1 \quad (6)$$

In terms of these projectors, microscopic operators S_A may be defined as

$$S_A = \sum_{i=1}^N S(i) P_A(i) \quad (7)$$

These sum to S , commute for $A \neq B$, and obey the commutation rules defining a spin operator. Further, $S_A \cdot S_B$ commutes with S^2 . Therefore, the local spin operators have most of the properties assumed for the phenomenological spin operators. We have previously discussed³ the evaluation of average values of $S_A \cdot S_B$ and the related average m_A of the net spin in the z direction associated with center A , S_{zA} , and the average N_A of the operator P_A .

For the special case of a spin-unrestricted single Slater determinant, $\langle S_A \cdot S_B \rangle$ is given by

$$\langle S_A \cdot S_B \rangle = -\frac{3}{8} B_{AB} + m_A m_B + \frac{1}{2} U_{AB} \quad (8)$$

for $A \neq B$, whereas for $A = B$

$$\langle S_A^2 \rangle = \frac{3}{8} \sum_{A \neq B} B_{AB} + m_A^2 + \frac{1}{2} F_A \quad (9)$$

Here, B_{AB} is the Wiberg–Mayer bond order,⁴ U_{AB} is the density of intrinsically delocalized spin,³ and F_A is the “free valence” (or “unpaired”) density⁴ on center A . Note that if $m_A^2 = S_A^2$ and $1/2 F_A = S_A$, then $\langle S_A^2 \rangle$ will differ from $S_A(S_A + 1)$ by the additional contribution by the bonding electron pairs. Similarly, if U_{AB} is zero, $\langle S_A \cdot S_B \rangle$ will differ from $m_A m_B$ by a covalent bond order contribution. As long as the B_{AB} contributions remain constant for all spin states within the family, the affect of B_{AB} on the Heisenberg Hamiltonian is to change E_0 in eq 1.

In this paper, we will choose $P_A = w_A(r_i)$ in eqs 5–7, where w_A is one inside a volume associated with atom A and zero outside. These volumes are chosen to be nonoverlapping and cover all of space. A point r is assigned to volume A if the ratio r_A/R_A is smaller than this ratio for any other center. The atomic radii R_A are chosen so that the atomic charges agree closely with the charges computed by Bader’s atoms in molecules (AIM) method.⁵

Previously, we considered complexes containing one and two Mn^{II} centers.³ Those results using the AIM volumes are similar to the results reported here for complexes with three and four Mn centers.

Computational Method

The focus of this paper is on the method for the spin and Heisenberg Hamiltonian analysis and not the exact results. Consequently, we examine simple model “butterfly” clusters that contain tetrahedral Mn centers. The energies and orbitals

were computed with the unrestricted B3LYP density functional (UB3LYP) method⁶ as implemented in Gaussian 98.⁷ The LANL2 pseudopotential and the LANL2DZ basis set were used for Mn.⁸ For the complex with three metal centers, **A**, the 6-31G* basis⁹ was used for O and H. For the complexes with four metal centers, **B** and **C**, the 6-31G* basis was used only for the two μ_3 bridging oxygens, and all other atoms had only a 6-31G basis.⁹ For the purpose of this paper, the DFT Kohn–Sham orbitals were used to form a Slater determinant that was then treated as an approximate wave function.

The local projectors were defined using the following atomic radii: 0.97 Å for O, 0.44 Å for H, and 0.99 Å for Mn. This radius for Mn generally results in populations that agree with the AIM populations for charges on the Mn between +2 and +3, because the volume around the Mn that originally contained the 4s orbital is assigned exclusively to the ligands, whereas the 3d region is assigned exclusively to the metal. In previous work,³ we found that the choice of the metal radius had a large effect on the computed net charge but only a small effect on the local spin properties.

Energies and Kohn–Sham determinants were computed with all singly occupied orbitals having “spin-up”. The number of orbitals to be singly occupied were chosen by chemical intuition to match the expected result for high-spin Mn centers with the nominal oxidation number (i.e., Mn^{II} $S = 5/2$ with five singly occupied d orbitals or Mn^{III} $S = 2$ with four singly occupied d orbitals). Convergence to the high M spin state was generally easy. The geometry was optimized for this situation, and then all other energies were computed as “vertical” energy differences for this fixed structure. The Mn d orbitals from the high M calculation were localized, and those on selected metal centers had their spins reversed to generate initial guesses for states with some metal centers having “spin-down”. With some effort, we were finally able to get converged energies and Kohn–Sham determinants corresponding to situations where each metal atom had $M_A = \pm S_A$ to a good approximation, but the actual signs of M_A spanned all possible combinations.

For each of these Kohn–Sham determinants we computed the expectation values in eqs 8 and 9 with the MELD suite of programs.¹⁰ Then eq 2 was solved for the J couplings using both the computed averages $\langle S_A \cdot S_B \rangle_X$ and the nominal values $M_A M_B$ with idealized values of M_A . A similar methodology, using idealized $\langle S_A \cdot S_B \rangle_X$, has been previously employed by Kortus and co-workers, as well as Raghu and co-workers.¹¹

We also optimized the structure of a complex with only two manganese centers, $(\mu_2\text{-OH})_2\text{Mn}_2\text{H}_2\text{O}(\text{OH})_3$ ($M = 9/2$) with the same DFT functionals and basis sets as the other three manganese complexes. A single point $M = 1/2$ DFT calculation was also performed. Subsequent 9 electron, 10 orbital CASSCF calculations for the $S = 9/2$ and the lowest energy $S = 1/2$ state were then performed with the same pseudopotential and basis sets using HONDO99 at the DFT $S = 9/2$ geometry.¹² The active space was composed of the 10 d orbitals of the two Mn centers, nine of which were singly occupied.

Results

The first complex considered, $\text{Mn}_3\text{O}(\text{OH})_4(\text{H}_2\text{O})_4$ which we label **A** in Figure 1, had three Mn^{II} centers with one $\mu_3\text{-O}$, a $\mu_2\text{-OH}$ group bridging Mn1 and Mn2, one additional OH ligand on each Mn, and enough H₂O ligands to make each Mn tetrahedral. The formal oxidation states are $5/3$ for Mn3 and $13/6$ for Mn1 and Mn2. The ground state of this system has five singly occupied d orbitals on each Mn with all five electrons coupled as high-spin $S = 5/2$. UB3LYP calculations were done

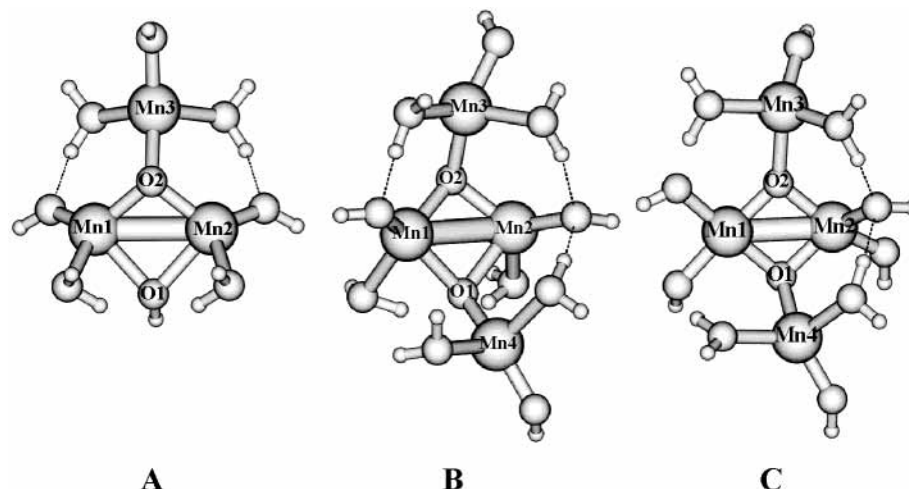


Figure 1. Numbering scheme for model complexes $\text{Mn}_3\text{O}(\text{OH})_4(\text{H}_2\text{O})_4$ (A), $\text{Mn}_4\text{O}_2(\text{OH})_4(\text{H}_2\text{O})_6$ (B), and $\text{Mn}_4\text{O}_2(\text{OH})_6(\text{H}_2\text{O})_4$ (C).

TABLE 1: Energies of Compounds A, B, and C Calculated by UB3LYP, with the LANL2 Pseudopotential and LANL2DZ Basis Set on Mn^a

A									
Mn ^{II} 1	Mn ^{II} 2	Mn ^{II} 3	energy	$\Delta E(\text{cm}^{-1})$	$\langle S^2 \rangle$	Mn–Mn	Mn–X	X–X	
↑	↑	↑	–996.3028157	0	63.8	56.9	4.2	2.7	
↓	↑	↑	–996.3052545	–535	13.7	13.9	–2.5	2.3	
↑	↓	↑	–996.3052545	–535	13.7	13.9	–2.5	2.3	
↑	↑	↓	–996.3055161	–593	13.7	13.9	–2.4	2.2	
B									
Mn ^{II} 1	Mn ^{II} 2	Mn ^{II} 3	Mn ^{II} 4	energy	$\Delta E(\text{cm}^{-1})$	$\langle S^2 \rangle$	Mn–Mn	Mn–X	X–X
↑	↑	↑	↑	–1328.266152	0	110.0	97.6	8.6	3.8
↑	↑	↑	↑	–1328.273667	–1649	34.9	32.9	–1.1	3.1
↑	↓	↑	↑	–1328.273746	–1667	34.9	33.0	–1.2	3.1
↑	↑	↓	↑	–1328.272486	–1390	35.0	32.9	–1.1	3.1
↑	↑	↑	↓	–1328.270301	–911	35.0	33.1	–1.2	3.1
↓	↓	↑	↑	–1328.275865	–2132	9.9	11.4	–4.4	2.9
↓	↑	↓	↑	1328.273835	–1686	9.9	11.4	–4.3	2.8
↓	↑	↑	↓	–1328.273813	–1681	9.9	11.4	–4.4	2.9
C									
Mn ^{III} 1	Mn ^{III} 2	Mn ^{III} 3	Mn ^{III} 4	energy	$\Delta E(\text{cm}^{-1})$	$\langle S^2 \rangle$	Mn–Mn	Mn–X	X–X
↑	↑	↑	↑	–1327.112538	0	90.1	81.7	4.1	4.2
↑	↑	↑	↑	–1327.116924	–963	34.0	32.4	–2.2	3.8
↑	↓	↑	↑	–1327.117456	–1079	34.0	32.9	–2.7	3.8
↑	↑	↓	↑	–1327.113359	–180	25.0	25.2	–3.8	3.6
↑	↑	↑	↓	–1327.114002	–321	25.0	25.0	–3.7	3.7
↓	↑	↑	↑	–1327.115199	–584	10.0	11.8	–5.4	3.6
↓	↑	↓	↑	–1327.116495	–868	9.0	11.0	–5.6	3.6
↓	↑	↑	↓	–1327.117572	–1105	9.0	11.0	–5.5	3.5

^a A utilized the 6-31G* basis set on O and H, whereas B and C only used the 6-31G* basis set on the bridging O's and the 6-31G basis on all other atoms.

with all 15 singly occupied orbitals having “spin-up”, and with all of the spins on one atom opposite to the other two atoms (hence, three different calculations). The energies given in Table 1 show that having the spin on Mn3 reversed from the other two gave the lowest single Slater determinant energy.

Table 1 also shows that the total $\langle S^2 \rangle_X$ is very close to the nominal values of 63.75 and 13.75 expected for these calculations. Table 2 presents $\langle S_A \cdot S_B \rangle$ and $\langle S_A^2 \rangle$ for the $M = 15/2$ and $5/2$ calculations. For the various M values, the average $\langle S_A^2 \rangle$ changed by less than 0.1, whereas the average $\langle S_A \cdot S_B \rangle$ changed sign but had little change in magnitude. The absolute value of $\langle S_{ZA} \rangle_X$ also changed by no more than 0.01 and remained close to the expected value of $5/2$. The calculated charge, q , on the metal centers was nearly unchanged between the different M calculations but is considerably smaller than the formal oxidation number for each Mn. Thus, aside from differences in the sign of $\langle S_A \cdot S_B \rangle$, the rest of the wave function remains unchanged

for this set of calculations and the conditions for use of the Heisenberg Hamiltonian are satisfied.

The source of the splitting in energy with the spin orientation on the atoms is not a through space interaction. Rather, coupling through the bridging oxygens is apparent in the observed changes in $\langle S_{Mn} \cdot S_O \rangle$ and in the extent of spin-polarization of these oxygens: for example, m_{O2} is 0.17 when M is $15/2$. For the case with all Mn “spins-up”, the product $m_{Mn2}m_{O2}$ contributes +0.39 to $\langle S_{Mn2} \cdot S_{O2} \rangle$, whereas the bond order term in eq 9 contributes –0.18, which corresponds to a net bond order of 0.5. Although the $\langle S_{Mn2} \cdot S_{O2} \rangle$ average becomes negative when one Mn is “spin-down”, the bond orders change very little. From Table 2, we observe that the total m contribution from all the ligand atoms is 0.55 when $M = 15/2$, but only 0.18 when M is $5/2$. We can then deduce that spin frustration of the Mn leads to spin polarization influences of opposite sign at the μ_3 -O, which cancel each other and lead to more delocalization of the unpaired

TABLE 2: Local Spin Results for Compound A, Obtained from UB3LYP with the LANL2 Pseudopotential and the LANL2DZ Basis Set on Mn and the 6-31G* Basis Set on O and H

	Mn ^{II} 1	Mn ^{II} 2	Mn ^{II} 3	μ_3 -O	μ_2 -OH
$\langle S_z \rangle$	2.32	2.32	2.31	0.17	0.06
q	1.32	1.32	1.34	-1.23	-1.36
$\langle S_A \cdot S_B \rangle$					
Mn ^{II} 1	8.25	5.37	5.36	0.21	0.05
Mn ^{II} 2		8.25	5.36	0.21	0.05
Mn ^{II} 3			8.21	0.24	0.14
$\langle S_z \rangle$	2.31	2.31	-2.30	0.07	0.06
$\langle S_A \cdot S_B \rangle$					
Mn ^{II} 1	8.20	5.33	-5.32	0.00	0.04
Mn ^{II} 2		8.20	-5.32	0.00	0.04
Mn ^{II} 3			8.13	-0.33	-0.13
$\langle S_z \rangle$	-2.30	2.31	2.31	0.04	0.00
$\langle S_A \cdot S_B \rangle$					
Mn ^{II} 1	8.12	-5.31	-5.30	-0.27	-0.09
Mn ^{II} 2		8.19	5.32	-0.09	-0.09
Mn ^{II} 3			8.18	-0.06	0.00

TABLE 3: Calculated J Values from Eq 2 from the UB3LYP Results for Compounds A, B, and C, Using the LANL2 Pseudopotential and LANL2DZ Basis Set on Mn^a

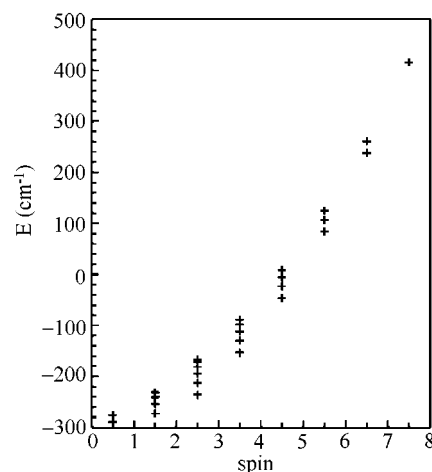
J	Mn1	Mn2	Mn3
	A		
Mn ^{II} 2	19(22)		
Mn ^{II} 3	24(28)	24(28)	
	B		
Mn ^{II} 2	47(56)		
Mn ^{II} 3	54(63)	50(58)	
Mn ^{II} 4	30(35)	36(42)	7(8)
	C		
Mn ^{III} 2	92(105)		
Mn ^{III} 3	14(16)	8(9)	
Mn ^{II} 4	9(10)	27(30)	-3(-4)

^a **A** utilized the 6-31G* basis set on O and H, whereas **B** and **C** only used the 6-31G* basis set on the bridging O's and the 6-31G basis on all other atoms.

spins between Mn and O. The latter is indicated by a small increase in the magnitude of Mn-(μ_3 -O) coupling, which in turn may be responsible for the slightly lower energy of the M of $5/2$ state than for the M of $15/2$ state.

The local spin properties of **A** are further examined in Table 1. There, column eight sums the $\langle S_A \cdot S_B \rangle_X$ terms between each set of Mn centers, $\sum_{A=Mn} \sum_{B=Mn} \langle S_A \cdot S_B \rangle$. In the high spin $M = 15/2$ calculation, this value is ferromagnetic and contributes 90% to the total $\langle S^2 \rangle$ of 63.8. Column nine, which sums the interaction with each Mn and every other atom except the remaining two Mn centers, $\sum_{A=Mn} \sum_{B \neq Mn} \langle S_A \cdot S_B \rangle$, and column ten, which sums the spin coupling between every atom (excluding Mn) with every other atom (excluding Mn), $\sum_{A=Mn} \sum_{B \neq Mn} \langle S_A \cdot S_B \rangle$, yield values that are net ferromagnetic and contribute 6.6% and 4.2%, respectively, to the total $\langle S^2 \rangle$ when $M = 15/2$. When one Mn is "spin-down" the spin coupling between Mn and the ligand atoms [dominated by $\langle S_{Mn} \cdot S_{O1, O2} \rangle$] becomes negative which in turn causes a decrease in the Mn-Mn coupling to 13.9, whereas the ligand-ligand spin coupling remains unchanged.

Two sets of J values were computed for **A** and are given in Table 3. One set of J couplings was derived assuming $\langle S_A \cdot S_B \rangle_X$ had the ideal value of ± 6.25 , whereas the other set (in parentheses) used the computed values near ± 5.3 . This choice results approximately in a simple scaling of the J value. When used in the Heisenberg Hamiltonian with idealized values of the atomic spins, it seems more consistent to use the J obtained

**Figure 2.** Distribution of spin states for compound **A** from the Heisenberg Hamiltonian using idealized $\langle S_A \cdot S_B \rangle_X$.**TABLE 4: Coefficients, C , for the Dominant Terms in the $S = 1/2$ Ground State of Compound A Expanded in the $|m_1 m_2 m_3\rangle$ States of the Atoms**

Mn ^{II} 1	Mn ^{II} 2	Mn ^{II} 3	C
-3/2	5/2	-1/2	0.25
-1/2	5/2	-3/2	-0.31
1/2	1/2	-1/2	-0.23
1/2	5/2	-5/2	0.28
3/2	3/2	-5/2	-0.36
5/2	-3/2	-1/2	0.25
5/2	-1/2	-3/2	-0.31
5/2	1/2	-5/2	0.28

from the idealized $\langle S_A \cdot S_B \rangle_X$ because it is implicitly assumed that $\langle S_A \cdot S_B \rangle_X$ has its ideal value in computing the matrix elements in the basis $|S_1, M_1, S_2, M_2, S_3, M_3\rangle$. Figure 2 shows the distribution of resulting spin states, with a ground state of $S = 1/2$. As shown in Table 4, the dominant term (which only accounts for 13% of the wave function) has $M = 3/2$ for Mn1 and Mn2 and $M = -5/2$ for Mn3. The $M = 3/2$ spin function for $S = 5/2$ is a linear combination with equal coefficients of the five Slater determinants that can be formed by flipping the spin of one of the five singly occupied d orbitals. Hence, this one term in the ground $S = 1/2$ state is already a linear combination of $5^2 = 25$ Slater determinants with equal coefficients.

The second model complex, $Mn_4O_2(OH)_4(H_2O)_6$ which we label **B** in Figure 1, was generated by replacing the H of the bridging OH group by Mn(OH)(OH)₂ and reoptimizing the structure. Hydrogen bonding between ligands on different centers causes **B** to have no symmetry. This "butterfly" complex then has wingtip Mn3 and Mn4 centers with formal charges of $5/3$ and backbone Mn1 and Mn2 with formal charges of $7/3$. Here, the lowest energy calculation still has five singly occupied d orbitals of the same spin on each Mn. Table 1 shows the eight possible energies for this structure having (a) all unpaired spins parallel so $M = 10$, (b) four ways to reverse the spin of one Mn so $M = 5$, and (c) three ways to have the spins of two Mn opposite to the other two so $M = 0$. All calculations give $\langle S^2 \rangle_X$ close to the ideal value of $M^2 + 10$. Table 5 gives the average values of $\langle S_A \cdot S_B \rangle_X$ for the $M = 10$ calculation and the lowest energy $M = 0$ calculation.

For **B**, there are seven parameters in eq 1, so we have fit eq 2 to seven of the energies in Table 1. Table 3 presents the resulting J values computed with both the idealized values of $\langle S_A \cdot S_B \rangle_X$ and the computed values (in parentheses). Again, the average values $\langle S_A \cdot S_B \rangle_X$ vary little in absolute value between the different spin combinations, so the results are merely scaled.

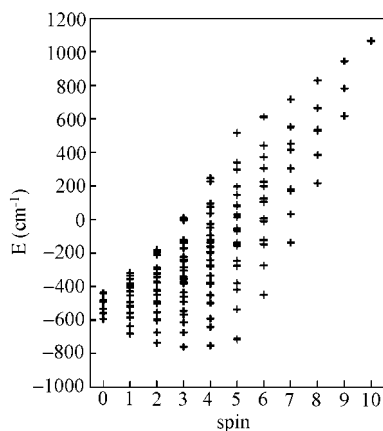


Figure 3. Distribution of spin states for compound **B** from the Heisenberg Hamiltonian using idealized $\langle S_A \cdot S_B \rangle_X$.

TABLE 5: Local Spin Results for Compound B, Obtained from UB3LYP with the LANL2 Pseudopotential and LANL2DZ Basis Set on Mn, the 6-31G* Basis Set on the μ_3 -O's, and the 6-31G Basis Set on All Other Atoms

	Mn ^{II} 1	Mn ^{II} 2	Mn ^{II} 3	Mn ^{II} 4	μ_3 -O(1)	μ_3 -O(2)
$\langle S_z \rangle$	2.32	2.32	2.33	2.32	0.17	0.13
q	1.29	1.28	1.35	1.35	-1.23	-1.35
Mn ^{II} 1	8.26	5.37	5.40	5.37	0.22	0.18
Mn ^{II} 2		8.26	5.40	5.37	0.20	0.18
Mn ^{II} 3			8.29	5.39	0.23	0.29
Mn ^{II} 4				8.22	0.39	0.12
$\langle S_z \rangle$	-2.31	-2.31	2.31	2.31	0.07	0.03
$\langle S_A \cdot S_B \rangle$						
Mn ^{II} 1	8.19	5.31	-5.33	-5.32	-0.01	-0.05
Mn ^{II} 2		8.20	-5.33	-5.32	-0.03	-0.04
Mn ^{II} 3			8.18	5.32	-0.33	-0.07
Mn ^{II} 4				8.18	-0.16	-0.24

TABLE 6: Coefficients, C , for the Dominant Terms in the $S = 3$ Ground State of Compound B Expanded in $|m_1 m_2 m_3 m_4\rangle$ States of the Atoms

Mn1	Mn2	Mn3	Mn4	C
-1/2	-3/2	5/2	5/2	0.21
1/2	-5/2	5/2	5/2	-0.33
3/2	-5/2	3/2	5/2	0.49
5/2	-5/2	1/2	5/2	-0.46
5/2	-3/2	-1/2	5/2	0.32

The J values from the idealized values of $\langle S_A \cdot S_B \rangle_X$ were used to compute the spectrum of the Heisenberg Hamiltonian. The results displayed pictorially in Figure 3 show that the ground state is $S = 3$ even though $M = 0$ for the best single determinant. Table 6 shows the dominant terms in this complicated $S = 3$ wave function for the case that $M = 3$. Using step-down operators on the $S = 3$ function, one can generate the $M = 2, 1, \dots, -2, -3$ wave functions, all with equal energy. The single configuration with all "spin-up" on Mn2 and Mn3 and all "spin-down" on Mn3 and Mn4 constitutes less than 0.05% of the $S = 3, M = 0$ wave function.

In the final example, $Mn_4O_2(OH)_6(H_2O)_4$ which we label **C** in Figure 1, the H_2O ligand on Mn1 and Mn2 was replaced by an OH. This changed Mn1 and Mn2 to Mn^{III} with four singly occupied d orbitals to yield two $S = 2$ centers, each with a formal charge of $^{10}/_3$. The energies and total spin for this complex are shown in Table 1. In **C**, the average $\langle S^2 \rangle_X$ differ by up to 1 from the ideal values of 90, 35, 26, 10, and 9, which indicates that the electronic structure changes somewhat for each spin solution and that this a poorer candidate for fitting by the Heisenberg Hamiltonian. Because of the nominally empty d orbital on the Mn^{III} center, it was possible that each spin

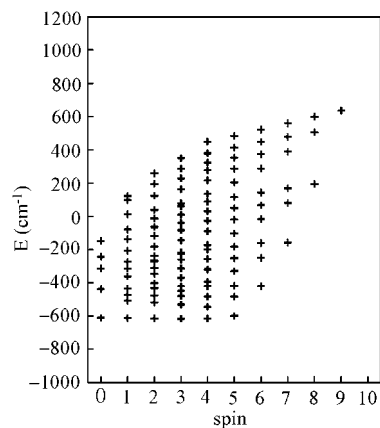


Figure 4. Distribution of spin states for compound **C** from the Heisenberg Hamiltonian using idealized $\langle S_A \cdot S_B \rangle_X$.

TABLE 7: Local Spin Results for Compound C Obtained from UB3LYP with the LANL2 Pseudopotential and LANL2DZ Basis Set on Mn, the 6-31G* Basis Set on μ_3 -O, and the 6-31G Basis Set on All Other Atoms

	Mn ^{III} 1	Mn ^{III} 2	Mn ^{II} 3	Mn ^{II} 4	μ_3 -O(1)	μ_3 -O(2)
$\langle S_z \rangle$	1.91	1.88	2.30	2.31	0.08	0.08
q	1.56	1.55	1.40	1.38	-1.09	-1.09
$\langle S_A \cdot S_B \rangle$						
Mn ^{III} 1	6.39	3.59	4.41	4.42	-0.07	-0.07
Mn ^{III} 2		6.23	4.32	4.33	-0.07	-0.08
Mn ^{II} 3			8.13	5.32	0.08	0.18
Mn ^{II} 4				8.17	0.19	0.07
$\langle S_z \rangle$	1.88	-1.86	-2.30	2.31	-0.02	0.01
$\langle S_A \cdot S_B \rangle$						
Mn ^{III} 1	6.26	-3.52	-4.35	4.35	-0.26	-0.19
Mn ^{III} 2		6.15	4.28	-4.30	-0.19	-0.25
Mn ^{II} 3			8.13	-5.32	-0.07	-0.03
Mn ^{II} 4				8.17	-0.04	-0.08

calculation could have a different orbital vacant. We verified that this did not happen and that the only change in the wave function was to flip all the spins using nearly the same orbitals. The calculated charges shown in Table 7 are slightly larger for the Mn^{III} centers than for the Mn^{II}. Interestingly, both the Mn^{III} and Mn^{II} charges in **C** are larger than the Mn^{II} charges in **B** as shown in Table 5. Further, the charges on the μ_3 -O's are less negative in **C** which illustrates the difficulty in supporting such a large formal charge on Mn^{III} by donating electrons to the bridging oxygens. Similar to **B**, the energy variation in the different spin solutions of **C** is related a slight increase in the delocalization of unpaired spin density and cancellation of the spin polarization at the bridging oxygens. It is interesting to note that in **C** for $M = 9$ the sum of the contributions to $\langle S^2 \rangle$ from the Mn-Mn spin coupling (column eight) is only 81.7 out of the total of 90.1 so that nearly 10% comes from the Mn-X (column nine) and X-X (column ten) spin interactions. For the next solution in Table 1, the sum over the Mn atoms in column eight is 32.4 so that only $\sim 5\%$ comes from the other spin couplings.

Table 3 gives the J values computed with both idealized and computed values (in parentheses) of $\langle S_A \cdot S_B \rangle_X$. The energy levels from the idealized J values are shown in Figure 4. Here, there is a slight preference for an intermediate spin ground state with total S of 3. Table 8 gives the wave function from the Heisenberg Hamiltonian for $S = 3$ and $M = 3$. The slightly dominant term in this expansion has $M = 2$ and -2 on the Mn1 and Mn2, but $M = 5/2$ and $1/2$ on the wingtips centers, Mn3 and Mn4. This agrees with the figure that is sometimes drawn for molecules

TABLE 8: Coefficients, C , for the Dominant Terms in the $S = 3$ Ground State of Compound C Expanded in $|m_1 m_2 m_3 m_4\rangle$ States of the Atoms

Mn ^{III} 1	Mn ^{III} 2	Mn ^{II} 3	Mn ^{II} 4	C
-2	2	5/2	1/2	0.23
-1	0	5/2	3/2	0.21
-1	1	3/2	3/2	0.20
-1	1	5/2	1/2	-0.22
0	-1	3/2	5/2	0.23
0	-1	5/2	3/2	-0.20
0	0	3/2	3/2	-0.25
1	-2	3/2	5/2	-0.24
1	-1	1/2	5/2	-0.24
1	-1	3/2	3/2	0.26
2	-2	1/2	5/2	0.35
2	-2	3/2	3/2	-0.23

of this type showing one of the spins pointing sideways rather than up or down.

Manganese Calculations with Multi Determinant Methods. For the case of a complex with only two transition metal centers, it is possible to perform CASSCF calculations of the eigenstates of S and M . For our purposes, we chose the mixed valent $(\mu_2\text{-OH})_2\text{Mn}_2\text{H}_2\text{O}(\text{OH})_3$ complex, with one Mn^{II} and one Mn^{III} center. Here, we used an arbitrary J value to solve the Heisenberg Hamiltonian and predict the wave function of each spin solution, because the relative energy of each solution is scaled linearly with J . This result was then compared with the CASSCF wave function to assess whether the Heisenberg assumption is valid for this model complex.

The 9 electron, 10 orbital CASSCF single-point calculation of the $S = 9/2$ wave function is almost entirely described ($\sim 99\%$) by a single Slater determinant composed of nine singly occupied orbitals on both Mn centers that are coupled as high spin. This is the same wave function as the one predicted by the Heisenberg Hamiltonian and DFT.

In contrast to the $S = 9/2$ state, the lowest energy $S = 1/2$, $M = 1/2$ state from the Heisenberg Hamiltonian is a linear combination of 126 Slater determinants, each with nine singly occupied orbitals. The single determinant with the largest coefficient ($\sim 25\%$) in the model wave function has $M = 5/2$ on Mn^{II} and $M = -2$ on Mn^{III}. This determinant becomes the lowest energy $M = 1/2$ solution in DFT, lying 139.9 cm^{-1} above the UB3LYP $S = 9/2$ spin state. The CAS wave function for the lowest energy $S = 1/2$ state is composed primarily ($\sim 94\%$) of determinants within the spin family that contains nine singly occupied orbitals. These determinants differ in which particular orbitals are “spin-up” and “spin-down”. Importantly, determinants that are not part of this spin family, e.g., those that doubly occupy the metal d orbitals or those that change which d orbital is singly occupied, do not contribute significantly to the CAS wave function. However, CAS and DFT do predict different orders for the $S = 9/2$ and $1/2$ states. The CAS results place the $S = 1/2$ state 5.4 cm^{-1} lower in energy than the $S = 9/2$ state.

Conclusion

The local spin quantities, $\langle S_A^2 \rangle$ and $\langle S_A \cdot S_B \rangle$, obtained from the Kohn–Sham Slater determinant of model manganese complexes differ from those suggested by chemical intuition by a bond order contribution. Using eq 2 to solve for the Heisenberg coupling constant J , we observe that the difference in ideal and calculated spin quantities merely results in a scaling of J . These quantities are also useful tools in assessing changes in a wave function for a variety of spin states, which makes it easier to assess whether the Heisenberg Hamiltonian approximation is valid for a model complex and approximate wave

function. It should always be recalled that the Heisenberg Hamiltonian models a family of states related by spin flipping, assuming no other changes in the wave function. It may well happen that the lowest energy low spin state is not related to the lowest energy high spin state by such a simple spin flipping relation.

Our DFT results indicate that some mixed valent metal complexes may experience small changes in the wave function for each single determinant spin solution, which would make them poorer candidates for fitting by the Heisenberg Hamiltonian. However, it is comforting that the CAS and DFT results are in reasonable agreement for the dinuclear Mn complex examined here.

Acknowledgment. This work was supported by Grant No. CHE-9982415 from the National Science Foundation.

References and Notes

- (1) See for example: Vincent, J. B.; Christmas, C.; Chang, H. R.; Li, Q.; Boyd, P. D. W.; Huffman, J. C.; Hendrickson, D. N.; Christou, G. *J. Am. Chem. Soc.* **1989**, *111*, 2086. Libby, E.; McCusker, J. K.; Schmitt, E. A.; Folting, K.; Hendrickson, D. N.; Christou, G. *Inorg. Chem.* **1991**, *30*, 3486. Wemple, M. W.; Tsai, H. L.; Wang, S.; Claude, J. P.; Streib, W. E.; Huffman, J. C.; Hendrickson, D. N.; Christou, G. *Inorg. Chem.* **1996**, *35*, 6437. Aubin, S. M. J.; Wemple, M. W.; Adams, D. M.; Tsai, H. L.; Huffman, J. C.; Christou, G.; Hendrickson, D. N. *J. Am. Chem. Soc.* **1996**, *118*, 7746. Castro, S. L.; Sun, Z.; Grant, C. M.; Bollinger, J. C.; Hendrickson, D. N.; Christou, G. *J. Am. Chem. Soc.* **1998**, *120*, 2365. Aromí, G.; Claude, J.; Knapp, M. J.; Huffman, J. C.; Hendrickson, D. N.; Christou, G. *J. Am. Chem. Soc.* **1998**, *120*, 2977. Aubin, S. M. J.; Dilley, N. R.; Pardi, L.; Krzystek, J.; Wemple, M. W.; Brunel, L.; Maple, M. B.; Christou, G.; Hendrickson, D. N. *J. Am. Chem. Soc.* **1998**, *120*, 4991. Aromí, G.; Knapp, M. J.; Claude, J.; Huffman, J. C.; Hendrickson, D. N.; Christou, G. *J. Am. Chem. Soc.* **1999**, *121*, 5489. Yoo, J.; Brechin, E. K.; Yamaguchi, A.; Nakano, M.; Huffman, J. C.; Maniero, A. L.; Brunel, L.; Awaga, K.; Ishimoto, H.; Christou, G.; Hendrickson, D. N. *Inorg. Chem.* **2000**, *39*, 3615. Albel, B.; El Fallah, M. S.; Ribas, J.; Folting, K.; Christou, G.; Hendrickson, D. N. *Inorg. Chem.* **2001**, *40*, 1037. Aubin, S. M. J.; Sun, Z.; Eppley, H. J.; Rumberger, E. M.; Guzei, I. A.; Folting, K.; Gantzel, P. K.; Rheingold, A. L.; Christou, G.; Hendrickson, D. N. *Inorg. Chem.* **2001**, *40*, 2127, and references therein.
- (2) Noodleman, L. *J. Chem. Phys.* **1981**, *74*, 5737. Noodleman, L.; Davidson, E. R. *J. Chem. Phys.* **1986**, *109*, 131. Noodleman, L.; Norman, J. G., Jr. *J. Chem. Phys.* **1979**, *70*, 4903.
- (3) Clark, A. E.; Davidson, E. R. *J. Chem. Phys.* **2001**, *115*, 7382. Davidson, E. R.; Clark, A. E. *J. Mol. Phys.* **2002**, *100*, 373.
- (4) Mayer, I. *Int. J. Quantum Chem.* **1986**, *29*, 73; *ibid.* **1986**, *29*, 477.
- (5) Biegler, F. W.; Nguyen-Dang, T. T.; Tal, Y.; Bader, R. F. W.; Duke, A. J. *J. Phys. B: Atom. Mol. Phys.* **1981**, *14*, 2739. Bader, R. F. W. *Atoms in Molecules: A Quantum Theory*; Oxford University Press: Oxford, U.K., 1990.
- (6) Becke, A. D. *J. Chem. Phys.* **1993**, *98*, 5648. Lee, C.; Yang, W.; Parr, R. G. *Phys. Rev. B.* **1988**, *37*, 785.
- (7) Frisch, M. J.; Trucks, G. W.; Schlegel, H. B.; Scuseria, G. E.; Robb, M. A.; Cheeseman, J. R.; Zakrzewski, V. G.; Montgomery, J. A., Jr.; Stratmann, R. E.; Burant, J. C.; Dapprich, S.; Millam, J. M.; Daniels, A. D.; Kudin, K. N.; Strain, M. C.; Farkas, O.; Tomasi, J.; Barone, V.; Cossi, M.; Cammi, R.; Mennucci, B.; Pomelli, C.; Adamo, C.; Clifford, S.; Ochterski, J.; Petersson, G. A.; Ayala, P. Y.; Cui, Q.; Morokuma, K.; Malick, D. K.; Rabuck, A. D.; Raghavachari, K.; Foresman, J. B.; Cioslowski, J.; Ortiz, J. V.; Stefanov, B. B.; Liu, G.; Liashenko, A.; Piskorz, P.; Komaromi, I.; Gomperts, R.; Martin, R. L.; Fox, D. J.; Keith, T.; Al-Laham, M. A.; Peng, C. Y.; Nanayakkara, A.; Gonzalez, C.; Challacombe, M.; Gill, P. M. W.; Johnson, B. G.; Chen, W.; Wong, M. W.; Andres, J. L.; Head-Gordon, M.; Replogle, E. S.; Pople, J. A. *Gaussian 98*, revision A.7; Gaussian, Inc.: Pittsburgh, PA, 1998.
- (8) Hay, P. J.; Wadt, W. R. *J. Chem. Phys.* **1985**, *82*, 284.
- (9) Hehre, W. J.; Ditchfield, R.; Pople, J. A. *J. Chem. Phys.* **1972**, *56*, 2257. Hariharan, P. C.; Pople, J. A. *Theor. Chim. Acta* **1973**, *28*, 213.
- (10) MELD is a set of electronic structure codes written originally by L. E. McMurchie, S. T. Elbert, S. R. Langhoff, and E. R. Davidson with extensive modification by D. Feller and D. C. Rawlings.
- (11) Kortus, J.; Kellberg, C. S.; Pederson, M. R. *Phys. Rev. Lett.* **2001**, *86*, 3400. Raghu, C.; Rudra, I.; Sen, D.; Ramesha, S. *Phys. Rev. B* **2001**, *64*, 064419.
- (12) Dupuis, M.; Marquez, A.; Davidson, E. R. *HONDO 99.6*; IBM Corporation: Kingston, NY, 1999.